Management Systems in Production Engineering

2024, Volume 32, Issue 3, pp. 428-437

Date of submission of the article to the Editor: 01/2024
Date of acceptance of the article by the Editor: 07/2024

DOI 10.2478/mspe-2024-0040

PREDICTING MECHANICAL STRENGTH AND OPTIMIZED PARAMETERS IN FDM-PRINTED POLYLACTIC ACID PARTS VIA ARTIFICIAL NEURAL NETWORKS AND DESIRABILITY ANALYSIS

Hind H. Abdulridha, Tahseen F. Abbas, Aqeel S. Bedan
University of Technology

Abstract:
Fused deposition modeling (FDM) is a commonly used additive manufacturing (AM) technique in both domestic and industrial end-product fabrications. It produces prototypes and parts with complex geometric designs, which has the major benefits of eliminating the need for expensive tooling and flexibility. However, the produced parts often face poor part strength due to anisotropic fabrication strategies. The printing procedure, the kind of material utilized, and the printing parameters all have a significant impact on the mechanical characteristics of the printed item. In order to predict the mechanical properties related to printed components made with the use of FDM and Polylactic Acid (PLA) material, this study concentrates on developing a prediction model utilizing Artificial Neural Networks (ANNs). This study used the Taguchi design of experiments technique, utilizing (L25) orthogonal array as well as a Neural Network (NN) method with two layers and 15 neurons. The effect of FDM parameters (layer thickness (mm), percentage of infill density, number of top/bottom layers, shell thickness (mm), and infill overlap percentage) on ultimate tensile and compressive strength (UTS and UCS) was examined through analysis of variance (ANOVA). With an ANOVA result of 67.183% and 40.198%, respectively, infill density percentage was found to be the most significant factor influencing UCS and UTS dependent on other parameters. The predicted results demonstrated valuable agreement with experimental values, with mean squared errors of (0.098) and (0.326) for UTS and UCS, respectively. The predictive model produces flexibility in selecting the optimal setting based on applications.

Key words: *FDM, PLA, process parameters, ANOVA, ANN*

INTRODUCTION

Fused deposition modeling (FDM) stands out among AM techniques, utilized for creating 3D parts for newly designed prototypes and difficult end-use components that conventional methods struggle to produce [1, 2]. A 3D Computer-Aided Design model guides the selective layer-by-layer material combination to construct the required component [3]. Materials like Acrylonitrile Butadiene Styrene (ABS) and Polylactic Acid (PLA), which are extruded from nozzle tips as components or support materials onto FDM machine-working platforms, are the most often used materials in non-metallic 3D printing [4, 5]. Initial boundaries are set using a stereolithography (STL) file and raster, with subsequent interior filling using a predetermined nozzle speed and temperature. The process is repeated until the finished model is produced, adding each layer atop the previous one [5]. Figure 1 shows the FDM technique, which creates 3D parts layer by layer straight from a CAD model.

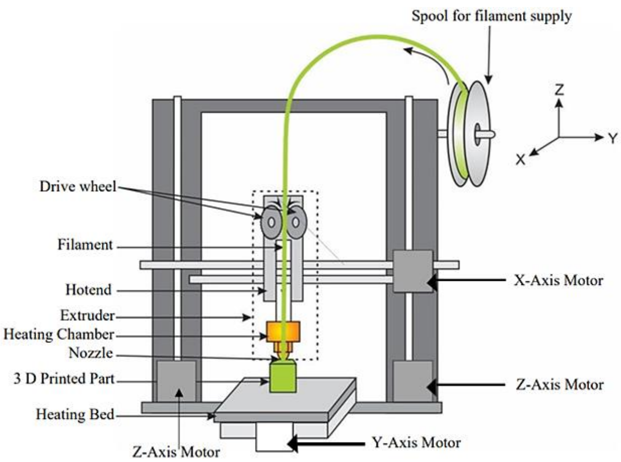

Fig. 1 Fused Deposition Modeling working principle
Source: [10].

It entails heating the material to a liquid state in a liquefier head and precisely depositing it using a nozzle that follows the cross-sectional geometry of the part [6].

While PLA is currently the most widely utilized material, elastomers, acrylonitrile butadiene styrene (ABS), medical-grade ABS thermoplastics, and polylactic acid PLA could also be utilized by FDMs for creating parts. A 1.75 mm diameter filament, wrapped onto spools, is the build and support material. The filament is fed via a flexible tube fastened to the back of the extrusion head, and the spools are mounted on a spindle situated on the machine's side or rear [4].

This work produces parts using the FDM technique with PLA filament. One of the commercially available materials for printing specimens is PLA, a bioactive and biodegradable polyester produced from lactic acid building blocks [7]. However, PLA has a drawback because it is brittle by nature. Since it doesn't need a heated bed and can be generated at low temperatures, it is the main filament used in the majority of extrusion-based 3D printers. PLA is incredibly inexpensive, easy to print, and yields parts with a wide range of uses [8]. Additionally, 3D printed PLA items have superior mechanical qualities to ABS [9].

Various FDM parameters significantly influence the quality of produced items. The optimal parameter set is believed to enhance 3D printed object quality and reduce production effort. Reference to the operating guide or the operator's experience and skills typically defines the required FDM process parameters. However, the results may not always be optimal for a specific system or environment. In such cases, the Taguchi approach emerges as a favorable alternative, providing functional simplicity and reducing the required number of experiments by predicting FDM parameters and their interactions [7].

Achieving the optimum process parameters is considered a continual task with the objective of minimizing production costs and satisfying product quality requirements. Mechanical properties are one of the most important performance characteristics in the FDM process. Higher mechanical characteristics are crucial for an effective FDM process, and these characteristics are considered to directly affect the hourly rate and the cost of production. Recently, researchers have been utilizing a variety of approaches, including artificial neural networks, genetic algorithms (GAs), simulated annealing, gray relational analysis, and others, to predict the responses and optimize printing parameters. Artificial Neural Networks (ANNs) are utilized for computation in addition to mapping relationships between input and output. Generalization, self-organization, and association are among the functions that ANN can perform in a way that is similar to those of the human brain. ANN is suitable for non-linear process modeling since it may approximate any function more effectively. ANNs have significant generalization and learning capabilities and are able to capture complicated relationships between input and output [11].

LITERATURE REVIEW

With the fundamental results of this kind of studies, the present work provides a detailed investigation into FDM technology’s performance characteristics. The effects of various parameters of FDM on part strength require more research [12, 13]. As such, it is highly important to understand the part's limitations prior to giving any recommendations for a particular application.

An experimental examination of the ANN model, parametric optimization, and PEEK 3D printing has been conducted by Borah and Chandrasekaran [14]. This research examined 4 process parameters, which are: printing speed PS, infill pattern, layer height, and infill density ID. For more sufficient strength and surface quality, a 4-12-2 network design ANN model with lower PS and higher ID requirements has been ideal. For the purpose of maximizing the dimensional characteristics in the FDM, Sivarao et al. [15] have created a NN model through utilizing some control elements like layer thickness, orientation, raster width, air gap, and raster angle. With percentage errors that range from 0.01% to 25.49% for the length, 4% at most for the thickness and 10% at most for the weight, the model was capable of correctly predicting dimensional parameters. Findings have demonstrated the way that the ANN may be utilized for optimizing FDM process parameters for higher dimensional accuracy, which would result in increasing the quality of the product as well as saving the costs of manufacturing.

A NN model has been created by Chinchanikar et al. [16] in order to predict FDM parts’ surface roughness. This model took into consideration infill density, print speed, nozzle temperature, hidden layers, layer height, and the number of neurons. This study found that 2 hidden layers, each with 150 neurons, had improved the accuracy of the prediction and that with the increase in infill density, surface roughness had decreased. Utilizing variance analysis, ANNs, and response surface methods, Monticeli et al. [17] provided modulus, flexural strength, and strain predictions for the high-performance 3D printable carbon fiber/epoxy composites. Vacuum pressure, curing temperature, printing speed, printing space, and thickness are some factors affecting AM composite processing. Low error rates and high reliability have been shown by the results, which also illustrate how efficiently and quickly composite materials with particular characteristics could be fabricated.

The effect of part orientation and process setting on the tensile strength in 3D printing has been studied by Milićević et al. [18]. For the purpose of creating correlations between the outputs and the inputs, an NN has been created. A hidden layer that includes 12 neurons was capable of producing the best results in terms of component orientation and process parameters where tensile strength had reached its maximal value. For the optimization, an ANN plays the role of a fitness function for a GA. Results have shown the potential of this method in the optimization of the 3D printing process, showing its potential in a variety of engineering areas. Gupta and Taufik [19] have proposed an innovative part strength modeling approach by utilizing ANNs for the reduction of prediction errors and improving 3D printed part strength predictions. The models that have been developed showed similar data trends for the ANN and RSM techniques; however, the RSM model had more errors. The ANN model is typically

precise; however, it is not suitable for smaller datasets. Based on the study, RSM and ANN could reduce the complications, minimize the number of required tests, and improve the MEAM process settings.
The effect of the 3D printing parameters on the dimensional deviations in the polylactic acid-printed parts has been researched by Abas et al. [20]. This study's results have shown that while the height of the layer had significant effects on the deviation of height and angle, infill density highly impacted the deviations in height and length. The desirability and weighted aggregated sum product assessment (WASPAS) integration provided optimal results, presenting a model for high-dimensional accuracy fabrication of the assistive devices. The NN models have been developed for the estimation of the effects of the primary FDM process parameters on the part quality with the ABS material, as stated by Tura et al. [21]. ANOVA and Taguchi L-9 orthogonal arrays have been utilized by the model for examining the way that the printing parameters impact surface roughness. Based on the research, orientation and infill angles had little bearing on the surface roughness; however, the thickness of the layer had the biggest impact.
It has been noted through a literature review that, through the proper modification of numerous associated parameters, the quality of parts that were generated using FDM can be enhanced. To create the highest-quality FDM part, it is crucial to identify the optimal parameter values using a structured approach since the mechanical properties are important output characteristics that are mostly crucial for the functionality and fitness of the components. However, according to an extensive literature review of several AM methods, FDM received the least attention. This study developed a feed-forward Neural Network (NN) with the use of a backpropagation (BP) algorithm for investigating the effects of the percentage of infill density, shell thickness (mm), layer thickness (mm), percentage of infill overlap, and number of top/bottom layers on the mechanical characteristics of printed specimens fabricated with the use of the FDM approach. The ANN model's prediction outputs have been the ultimate tensile strength (UTS) and ultimate compression strength (UCS). A system that could continuously control several parameters is eventually produced by creating an ANN model with several outputs and inputs.

METHODOLOGY

Experimental Work

Designing the part or component using design tools is the first stage in the 3D printing process. The SOLIDWORKS 2022 program prepares the computer-aided design (CAD) file. In addition, the 3D model must be transformed into a standard format after being obtained, regardless of the method. STL is the most often used file type extension. This file format is widely used and works with various platforms and devices. The model then needs to be translated into the preferred 3D printing language. G-Code is the most widely used language, particularly for printers of the FDM type. This code instructs the target machine to travel in different directions and at varying speeds, to change the temperature of its components, to activate its cooling components, and to carry out several other tasks [22]. Figure 2 depicts the workflow for this work, which begins with selecting FDM parameters and ends with calculating the percentage error between predicted and measured values.

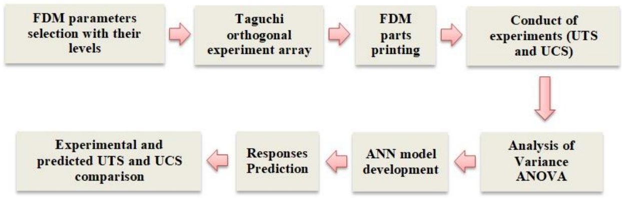

Fig. 2 Proposed work flow

Ultimaker Cura 4.13.1 is the software used for advanced slicing. The CAD model and the sliced model for the compressive and tensile specimens, respectively, are shown in Figure 3a, b.

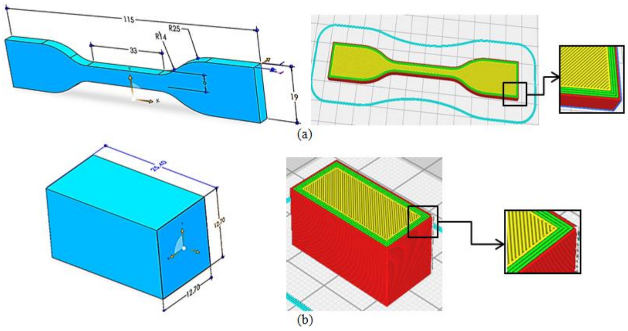

Fig. 3 Computer-Aided-Design and sliced models for (a) tensile specimen, (b) compressive specimen

Process parameter selection significantly affects the quality of a part produced with Fused Deposition Modeling (FDM). The process parameters investigated in this work are the percentage of infill density, shell thickness, layer thickness, percentage of infill overlap, and number of top/bottom layers. The performance of the FDM process, including tensile and compressive strength, is significantly influenced by variations in FDM parameters. As a result, optimal FDM parameter selection may lead to better FDM process performance. Table 1 displays the process parameters used to print the parts, while Table 2 shows that other FDM parameters are maintained at their fixed levels.

Table 1
The process parameters selected and their levels

Parameters	Levels				
	1	2	3	4	5
Infill Density %	30	40	50	60	70
Layer thickness (mm)	0.1	0.15	0.2	0.25	0.3
Shell thickness (mm)	1.2	1.6	2	2.4	2.8
Top/bottom layers number	3	4	5	6	7
Infill overlap %	10	15	20	25	30

Table 2
The fixed level of remaining FDM parameters

Parameters	Value	Units
Printing speed	80	mm/sec
Infill pattern	Cubic	-
Printing temperature	200	Degree Celsius
Build plate temperature	50	Degree Celsius

The experience, literature review, parameter significance and relevance as determined by early experimental investigations, and the recommended acceptable high and low levels from equipment manufacturers were all considered when selecting the FDM parameter levels. Three or more parameter levels are preferred to represent the response variables' behavior accurately. The experiments were conducted by employing the Taguchi experiment design. The tensile test is carried out following ASTM D638 type-4, while compressive testing is carried out following ASTM D-695.

For determining whatever performance characteristic deviates from the desired value, the Taguchi technique uses the S/N ratio. Performance characteristics are sometimes categorized as nominal-the-better, higher-the-better, and lower-the-better when analyzing the signal-to-noise ratio [23]. Maximum mechanical characteristics (strength) are required for optimal FDM performance. Consequently, it is best to have higher the better mechanical characteristics. Equation 1 could be used for calculating the signal-to-noise ratio (S/N):

$$S/N = -10\ log(\frac{1}{n}\sum_{k=1}^{n}\frac{1}{y_k^2}) \quad (1)$$

Where n represent the number of tests, y_k represent the value of the performance characteristics. The SolidWorks-designed specimens for the tensile and compressive testing were imported into the Ultimaker Cura 14.3.1 slicing software when the experiment design was completed. The generated G-code was then transferred to the Creality Ender-5 Pro 3D printer, which is illustrated in Figure 4.

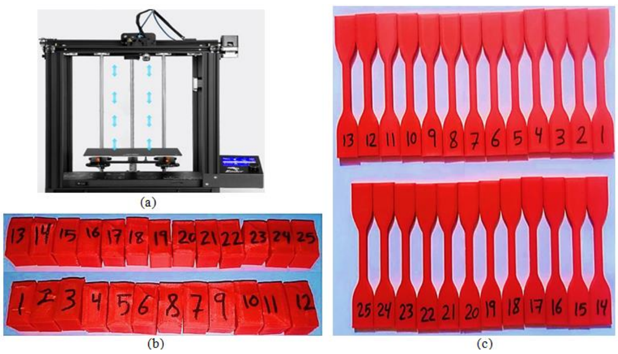

Fig. 4 Test specimens printing process, (a) Creality Ender-5 Pro 3D printer, (b) compressive specimens, (c) tensile specimens

Subsequently, TORWELL PLA filament material was utilized to fabricate the specimens through the 3D printing process. At room temperature, the mechanical characteristics of the printed specimens were evaluated using the WDW-200E computer-controlled electronic universal testing machine, as illustrated in Figure 5.

Fig. 5 Mechanical Tests at the WDW-200E Computer Controlled Electronic Universal Testing Machine

The testing apparatus is located at the Production Engineering and Metallurgy Department, University of Technology-Baghdad, Iraq. The testing procedures, which complied with a crosshead speed of 1.5 mm/min, adhered to the ASTM D638 type 4 and ASTM D695 standards for tensile and compressive testing, respectively. Thorough records of load, deformation, time, and stroke were diligently recorded during the examinations. In comparison with the CAD model, stress and mechanical characteristics were calculated using each specimen's measured dimensions. The UTS and UCS for each PLA test specimen might be more easily calculated utilizing Equation 2 with the recorded data.

$$\sigma = F/A \quad (2)$$

where:
σ represents the tensile and compressive stress in (N/mm^2),
F represents the applied force in (N),
A represents the cross-sectional area of the printed specimen in (mm^2).

Artificial Neural Network Prediction Model

A computational model called an artificial neural network (ANN) is modeled based on the biological neural networks (NNs) seen in the human brain. These are made up of "neurons," or nodes resembling neurons, stacked in layers. An input layer, hidden layers, and an output layer make up the layers in most cases. Information travels across the network via a training process that adjusts the weights on connections across neurons. Several sets of input data are first fed into the network, and then the system uses the errors produced by comparing the predicted and actual outcomes to adjust the weight values [24, 25, 26].

In this work, five input neurons (layer thickness (mm), percentage of infill density, number of top/bottom layers, shell thickness (mm), and percentage of infill overlap) with a (5x25) matrix of input data and two output neurons (UCS and UCS) with a (2x25) matrix of output data comprise the Hebbian learning rule in the NN model. These input and output neurons were introduced into the neural fitting tool, as shown in Figure 6.

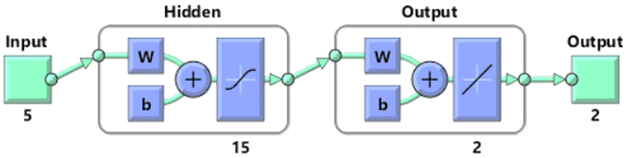

Fig. 6 Illustration of the employed neural network architecture

Desirability analysis

Desirability analysis (DA) is an effective statistical method utilized to evaluate and optimize several responses or parameters. Applications of desirability analysis may be found in many domains, including manufacturing, process optimization, and product design. These applications help to improve decision-making and overall performance. It offers a uniform structure for assessing the desirability of various results and determining the best combination of input parameters to maximize or minimize a variety of objectives.

Each objective is given a desirability function, and the objective values are mapped to a scale from 0 to 1, representing the desirability of each level, which combines with an overall desirability function for each combination of input parameters. Di = 1 means the response can be optimized; if it cannot, Di = 0 means it is not within an acceptable range. The "lower the better" or "higher the better" criterion determines the desirability values of responses; in the current instance, the value y is expected to be either lowest or maximum. When the desirability value Di increases beyond a threshold, it equals 0; when it goes below a threshold, it equals 1. The value of Di is a number between 0 and 1. The desirability function is derived from equations (3-5) for higher-the-better requirements. Equation 6 is used to evaluate overall desirability (Do) for the optimization that includes multiple response characteristics while taking individual desirability and its weight into account [14].

Higher-The-Better

$$y \geq y_{max};\ D_i = 1 \tag{3}$$

$$y_{min} \leq y \leq y_{max};\ D_i = \left[\frac{y - y_{min}}{y_{max} - y_{min}}\right]^r \tag{4}$$

$$y \leq y_{min};\ D_i = 0 \tag{5}$$

$$D_o = (D_1 w_1 * D_2 w_2 \ldots\ldots D_n w_n)^{(1/\sum w_i)} \tag{6}$$

where:
r represents the index of desirability,
y_{max} and y_{min} represent upper and lower limit of *y*.

RESULTS AND DISCUSSION

Analysis the results

The mechanical characteristics (UTS and UCS) of 25 FDM specimens were measured after the printing process, as presented in Table 3.

The results of the experiment are analyzed using Minitab 17. The best parameter level can be predicted by analyzing UTS and UCS results. An analysis of the relative contributions of several parameters is done using a statistical ANOVA in order to identify which parameters significantly affect the performance characteristics as well as how they interact.

Table 3
The experimental results

No.	Infill density %	Layer thickness(mm)	Shell thickness (mm)	Top/bottom layer no.	Infill overlap%	UTS (N/mm²)	UCS (N/mm²)
1	30	0.10	1.2	3	10	25.461	24.227
2	30	0.15	1.6	4	15	32.000	30.214
3	30	0.20	2.0	5	20	36.394	36.031
4	30	0.25	2.4	6	25	43.758	40.232
5	30	0.30	2.8	7	30	42.533	37.293
6	40	0.10	1.6	5	25	32.406	26.779
7	40	0.15	2.0	6	30	38.481	40.432
8	40	0.20	2.4	7	10	50.000	43.741
9	40	0.25	2.8	3	15	44.186	42.768
10	40	0.30	1.2	4	20	36.597	28.587
11	50	0.10	2.0	7	15	43.872	41.468
12	50	0.15	2.4	3	20	48.288	41.318
13	50	0.20	2.8	4	25	44.223	45.818
14	50	0.25	1.2	5	30	36.085	36.161
15	50	0.30	1.6	6	10	43.831	40.533
16	60	0.10	2.4	4	30	46.764	47.053
17	60	0.15	2.8	5	10	63.185	49.455
18	60	0.20	1.2	6	15	57.547	42.983
19	60	0.25	1.6	7	20	62.207	48.068
20	60	0.30	2.0	3	25	37.311	45.453
21	70	0.10	2.8	6	20	46.415	60.481
22	70	0.15	1.2	7	25	38.538	49.471
23	70	0.20	1.6	3	30	35.372	47.583
24	70	0.25	2.0	4	10	41.576	51.886
25	70	0.30	2.4	5	15	54.669	57.746

Depending on Table 3, the tensile strength has been experimentally increased from 25.5 MPa to 63 MPa in a specimen printed with infill density at level 4 = 60%, shell thickness at level 5 = 2.8 mm, layer thickness at level 2 = 0.15 mm, infill overlaps at level 1 = 10%, and number of top/bottom layers at level 3 = 5. It is important to notice that reference [27] states that the specimen's expected maximum tensile strength is 55 MPa. Conversely, compressive strength was experimentally increased from 24 MPa to 60.5 MPa in a specimen printed with infill density at level 5 = 70%, shell thickness at level 5 = 2.8 mm, layer thickness at level 1 = 0.1 mm, infill overlap at level 3 = 20%, and number of top/bottom layers at level 4 = 6. The reference [28] evaluated the specimen's predicted maximum tensile strength to be 55 MPa, which is significant.

Depending on the experimental data in Table 3, an ANOVA was used to establish the important parameters and interactions for UCS and UTS, which are presented in Table 4.

Table 4
ANOVA for UTS and UCS results

ANOVA for UTS						
Source	**DF**	**Adj SS**	**Adj MS**	**F-Value**	**P-Value**	**Percentage of contribution**
Infill density %	4	818.62	204.66	10.02	0.023	40.198
Layer thickness (mm)	4	132.30	33.07	1.62	0.326	6.497
Shell thickness (mm)	4	454.37	113.59	5.56	0.063	22.312
Top/bottom layer numbers	4	310.71	77.68	3.80	0.112	15.257
Infill overlap %	4	238.81	59.70	2.92	0.162	11.727
Error	4	81.67	20.42			4.01
Total	24	2036.48				
ANOVA for UCS						
Source	**DF**	**Adj SS**	**Adj MS**	**F-Value**	**P-Value**	**Percentage of contribution**
Infill density %	4	1268.84	317.210	30.82	0.003	67.183
Layer thickness (mm)	4	43.02	10.754	1.04	0.484	2.277
Shell thickness (mm)	4	438.09	109.521	10.64	0.021	23.196
Top/bottom layer numbers	4	88.02	22.004	2.14	0.240	4.661
Infill overlap %	4	9.50	2.376	0.23	0.908	0.503
Error	4	41.17	10.292			2.18
Total	24	1888.62				

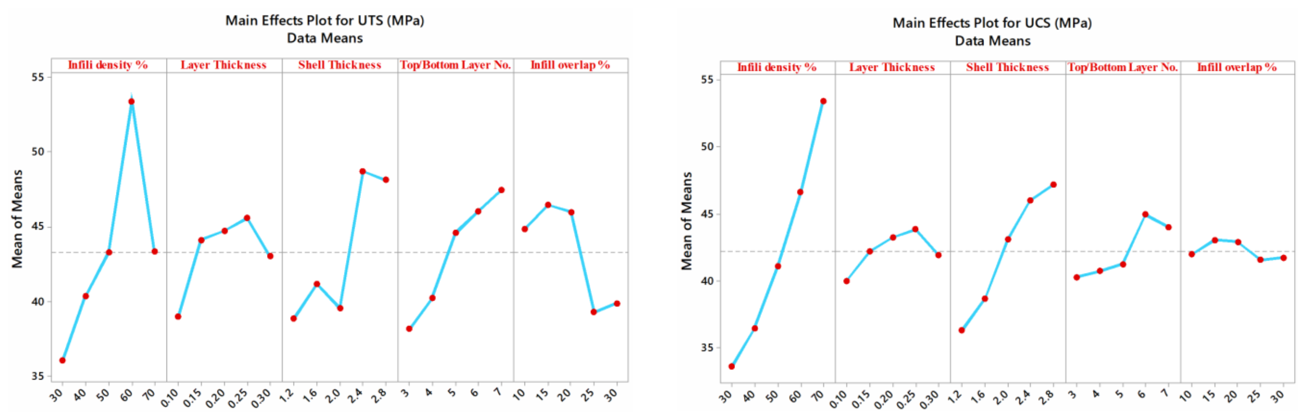

a) b)

Fig. 7 Main effect plot for (a) Ultimate tensile strength, (b) Ultimate compressive strengt

At a 95% confidence level and P-value of 0.023 and 0.003, respectively, Table 4 shows that infill density is the most important parameter affecting UTS and UCS, as can be seen in Figure 7 (a and b). The quantity of material utilized to fill the interior space of a 3D printed object is referred to as infill density. Since they need more material to sustain compressive stresses, components with higher infill densities are often stronger. It is evident that the specimen printed with a 30% infill density has a tensile strength (25 MPa) roughly three times lower than the specimen with a 60% infill density (63 MPa). The highest compressive and tensile strengths could be obtained with an infill density of 60% or 70%. However, the increase in the printing time and consumption of material may result in higher costs. Thus, it could be crucial to ascertain the required infill density based on the type of product and intended use.

The impact of the investigated parameters could be ascertained by calculating the percentage contribution of each parameter to the overall variation in the experimental results. This study shows that the percentage of infill density has the greatest influence on compressive and tensile strength, contributing 40.198% and 67.183%, respectively, with a 95% confidence level. Table 5 displays the optimal value and significance of each parameter.

Table 5
Optimum level and the significant for each parameter

Parameters	Optimized UTS	Optimized UCS
Infill density %	60%	70%
Layer thickness (mm)	0.25 mm	0.25 mm
Shell thickness (mm)	2.4 mm	2.8 mm
Top/bottom layer numbers	7	6
Infill overlap %	15%	15%
Significant	Infill density %	Infill density %, shell thickness

Where DF represents the degree of freedom, Adj SS represents the adjusted summation of squares, and Adj MS represents the adjusted mean squares.

Results of the developed ANN

Artificial neural network (ANN) is utilized to predict models that can be compared to experimental data. The neural network is trained using the experimental database. The ANN model was tested using the training set of data.

About 15% of the data is employed to test the model; an additional 15% is utilized for validating the model; and the remaining 70% is utilized for training the model. Table 6 illustrates the typical output response observation. The optimum choice for this work is thought to have been reached at epoch 0, as indicated in Figure 8, where the data yields the lowest mean absolute prediction error of 0.008108.

Table 6

The output response observation

Network Configuration	5 – 15 – 2
The transfer function type	Trainlm
Number of epochs	100
The learning rate factor (α)	0.001
Size of neuron	15
Size of layers	2
Number of training trails	17
Number of testing trails	4

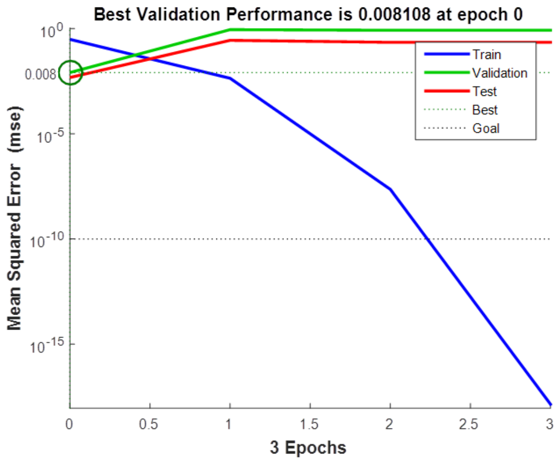

Fig. 8 Ultimate tensile and compressive strength performance plot

Figure 9 displays a simplified representation of the suggested system.

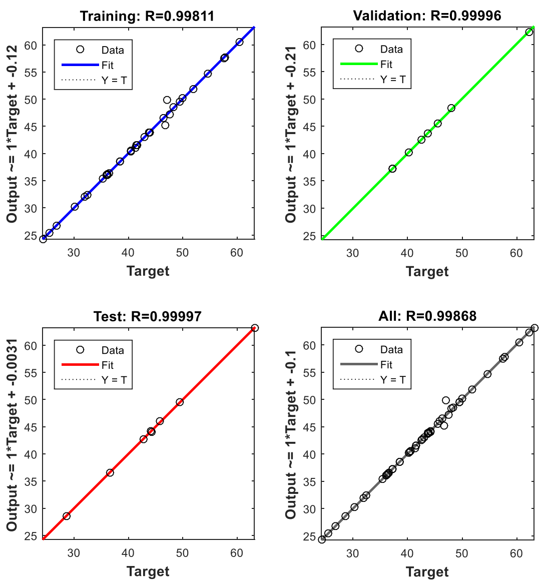

Fig. 9 The proposed network graphical representation

The Levenberg-Marquardt method generated the best results overall (R = 0.99868). The regression coefficient of the validation data set (R = 0.99996), which is near 1, shows a significant correlation between the ANN and experimental results. Equation 7 estimates the mean square error value [29].

$$MSE = \frac{1}{n}\sum_{t=1}^{n}(measured\ value - predicted\ value)^2 \quad (7)$$

Table 7 compares the ANN predicted and the experimental values for the tensile and compressive strength of PLA parts based on Equation 8. Table 7 shows that the maximum percentage error values were 3.257% and 5.970%, respectively, between the measured and predicted UTS and UCS.

Table 7

ANN results vs. experimental values for UTS and UCS

No.	UTS (N/mm^2)	Predicted UTS by ANN	Error %	UCS (N/mm^2)	Predicted UCS by ANN	Error %
1	25.461	25.460	0.003	24.227	24.222	0.020
2	32.000	32.000	0.001	30.214	30.212	0.007
3	36.394	36.396	0.006	36.031	36.031	0.001
4	43.758	43.758	0.000	40.232	40.232	0.001
5	42.533	42.533	0.000	37.293	37.293	0.000
6	32.406	32.407	0.004	26.779	26.778	0.002
7	38.481	38.481	0.000	40.432	40.432	0.001
8	50.000	50.221	0.442	43.741	43.915	0.398
9	44.186	44.187	0.003	42.768	42.768	0.000
10	36.597	36.605	0.021	28.587	28.590	0.009
11	43.872	43.873	0.003	41.468	41.470	0.004
12	48.288	48.478	0.394	41.318	41.117	0.485
13	44.223	44.104	0.270	45.818	45.972	0.335
14	36.085	36.086	0.002	36.161	36.161	0.001
15	43.831	43.831	0.001	40.533	40.533	0.000
16	46.764	45.241	3.257	47.053	49.862	5.970
17	63.185	63.185	0.000	49.455	49.455	0.000
18	57.547	57.547	0.001	42.983	42.984	0.003
19	62.207	62.309	0.163	48.068	48.302	0.486
20	37.311	37.312	0.002	45.453	45.454	0.003
21	46.415	46.534	0.256	60.481	60.532	0.084
22	38.538	38.538	0.001	49.471	49.471	0.000
23	35.372	35.336	0.103	47.583	47.251	0.698
24	41.576	41.576	0.001	51.886	51.886	0.000
25	54.669	54.669	0.000	57.746	57.746	0.000

The discrepancy between the experimental and predicted ANN model results is shown in Figures 10 and 11.

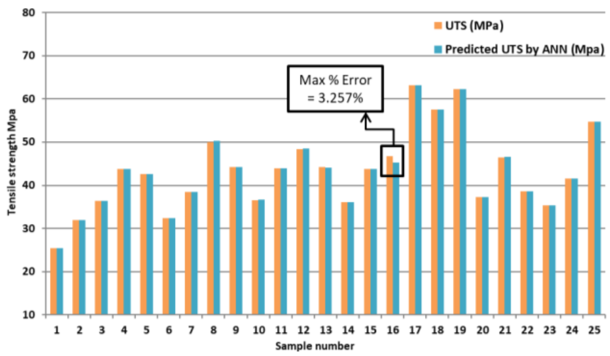

Fig. 10 Comparison between experimental vs. artificial neural network predicted values for ultimate tensile strength

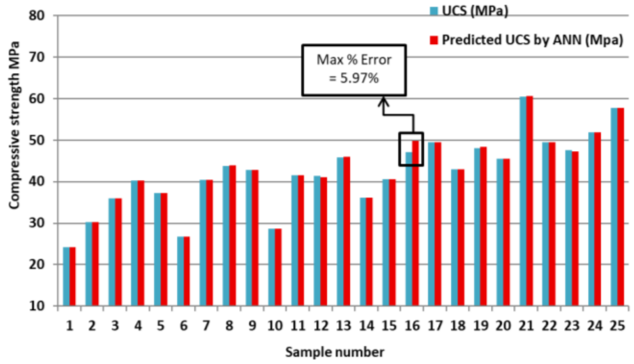

Fig. 11 Comparison between experimental vs. artificial neural network predicted values for ultimate compressive strength

The resultant percentage error, as illustrated in Figure 12, is acceptable, indicating that the ANN model has satisfactorily predicted UTS and UCS.

Error % = |((measured value — Predicted value)/measured value)·100| (8)

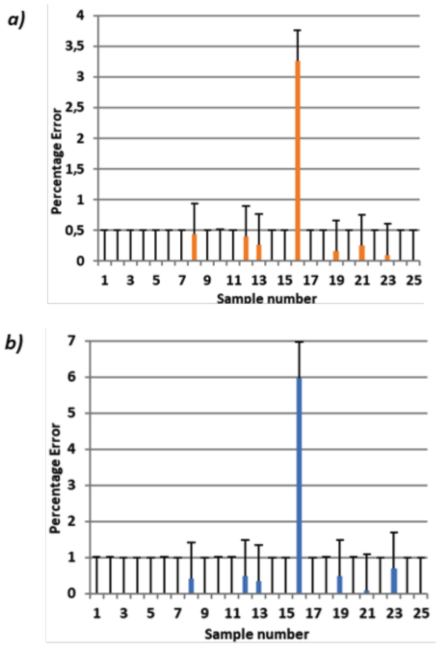

Fig. 12 Percentage error between experimental and predicted results for (a) tensile strength, (b) compressive strength

Optimized Results

The current study also employed a desirability analysis to optimize printing parameters. As shown in Figure 13, Minitab 17 is used to calculate the optimum printing parameters that produce the highest tensile and compressive strength.

It is essential to optimize every response simultaneously because the optimum parameters for individual responses tend to contract with each other. A composite desirability value of 0.9454 was obtained by multi-optimizing all parameters simultaneously using desirability analysis (DA). The optimal parameters included a 60% infill density percentage, 0.25 mm layer thickness, 2.8 mm shell thickness, 0.15 infill overlap, and six top/bottom layer numbers.

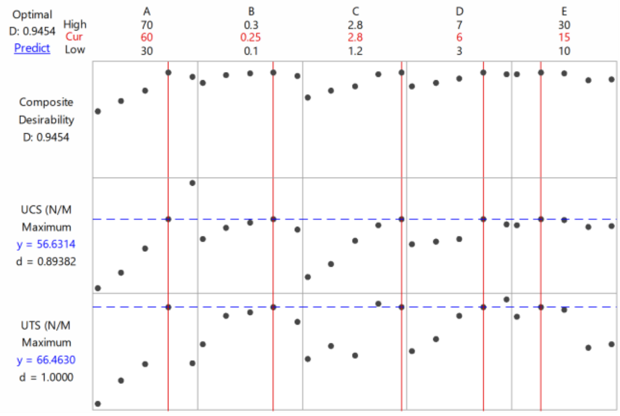

Fig. 13 Optimization of multi-responses (tensile and compressive strength) using desirability analysis

The related optimal responses have maximum UCS and UTS of 56.6314 and 66.463 MPa, respectively.

CONCLUSIONS

In this study, an Artificial Neural Network (ANN) model was developed for quantitatively predicting the mechanical properties of specimens made with FDM. The optimum FDM parameters (shell thickness, infill density percentage, number of top/bottom layers, layer thickness, and percentage of infill overlap) for tensile as well as compressive strength (UTS and UCS) were determined with the use of the desirability analysis DA technique. Some of the most significant conclusions are drawn as follows:

1. From the experimental results of the printed specimens' mechanical characteristics, the tensile strength of parts with a value of 63 MPa is optimized by a higher percentage of infill density of 60%, 0.8 mm shell thicknesses, 0.15 mm layer thicknesses, five top and bottom layers, and 10% infill overlap. However, the compression strength of the parts was optimized to 60.5 MPa by combining several parameters, such as 0.1 mm layer thickness, 70% infill density, 2.8 mm shell thickness, six top and bottom layers, and 20% infill overlap.
2. The ANOVA results indicate that the percentage of infill density was the most significant parameter for UTS and UCS, contributing 40.198% and 67.183% of the total, respectively.
3. ANN was used to learn the experimental data. A total of 17 patterns have been used to train the neural network (NN). Figures 10 and 11 show that the neural network model displays closed findings matching the predicted output model and the experimentally calculated UTS and UCS.
4. From the desirability analysis DA, the optimal UTS and UCS values were 66.5 MPa and 56.6 MPa, respectively. This was achieved with an infill density of 60%, a shell thickness of 2.8 mm, a layer thickness of 0.25 mm, six top/bottom layers, and 15% infill overlap.
5. By comparing the experimental and predicted values for UTS and UCS with the ANN model, it was discovered that the higher percentage errors for UTS and UCS were 3.257% and 5.97%, respectively. Nevertheless, this mistake can be further reduced if the number of test patterns increases.

REFERENCES

[1] S. Fafenrot, N. Grimmelsmann, M. Wortmann, and A. Ehrmann, "Three-dimensional (3D) printing of polymer-metal hybrid materials by fused deposition modeling," *Materials*, vol. 10, 2017, pp. 1199. https://doi.org/10.3390/ma10101199

[2] S. M. Ahmad and S. Y. Ezdeen, "Effect of coating on the specific properties and damping loss parameter of ultem 1010," *Zanco J. Pure Appl, Sci.*, vol. 33, 2021, pp. 105-116. https://doi.org/10.21271/ZJPAS.33.2.10

[3] T. Abbas, F. M. Othman, and H. B. Ali, "Effect of infill Parameter on compression property in FDM Process," *Dimensions*, vol. 12, 2017, pp. 24-25. https://doi.org/10.9790/9622-0710021619

[4] F. A. Naser and M. T. Rashid, "The Influence of Concave Pectoral Fin Morphology in the Performance of Labriform Swimming Robot," *Iraqi J. Electr. Electron. Eng.*, vol. 16, 2020, pp. 54-61. https://doi.org/10.37917/ijeee.16.1.7

[5] A.K. Sood, R.K. Ohdar, S.S. Mahapatra, "Improving dimensional accuracy of fused deposition modeling processed part using grey Taguchi method," *Mater Des*, vol. 30, no. 10, 2009, pp. 4243-4252. https://doi.org/10.1016/j.matdes.2009.04.030

[6] K. Kun, "Reconstruction and development of a 3D printer using FDM technology," *Procedia Engineering*, vol. 149, 2016, pp. 203-211. https://doi.org/10.1016/j.proeng.2016.06.657

[7] N.A. Aldeen, B.A. Sadkhan, and B. Owaid, "Hand bone orthosis manufacturing using 3d printing technology," *J. Eng. Sustain. Dev.*, vol. 24, 2020, pp. 451-458. https://doi.org/10.31272/jeasd.conf.1.50

[8] Y.F. Buys, A.N.A. Aznan, and H. Anuar, "Mechanical properties, morphology, and hydrolytic degradation behavior of polylactic acid/natural rubber blends," in *IOP Conference Series: Materials Science and Engineering*, vol. 290, 2018, p. 012077. https://doi.org/10.1088/1757-899X/290/1/012077

[9] M. Rismalia, S.C. Hidajat, I.G.R. Permana, B. Hadisujoto, M. Muslimin, and F. Triawan, "Infill pattern and density effects on the tensile properties of 3D printed PLA material," in *Journal of Physics: Conference Series*, vol. 1402, 2019, p. 44041. https://doi.org/10.1088/1742-6596/1402/4/044041

[10] T. Raj. "Investigation of Parameter-Property Relationship in Material Extrusion Additive Manufacturing." PhD thesis, Department of Mechanical Engineering, Faculty of Engineering Dayalbagh Educational Institute, Dayalbagh, Agra (UP) – 282005, 2023.

[11] B. Das, S. Roy, R.N. Rai, and S.C. Saha, "Studies on effect of cutting parameters on surface roughness of Al- Cu-Tic Mmcs: An Artificial Neural Network Approach," *International Conference on Advanced Computing Technologies and Applications*, 2015, pp. 745-752. http://doi.org/10.1016/j.procs.2015.03.145

[12] N. Hopkinson, R. Hague, and P. Dickens. Rapid Manufacturing: An Industrial Revolution for the Digital Age. *Wiley*, England, 2005.

[13] A. Pilipović, P. Raos, and M. Šercer, "Experimental analysis of properties of materials for rapid prototyping," *The International Journal of Advanced Manufacturing Technology*, vol. 40, 2009, pp. 105-115. https://doi.org/10.1007/s00170-007-1310-7

[14] J. Borah and M. Chandrasekaran, "Experimental investigation and development of Artificial neural network modeling of 3D printed PEEK bio implants and its optimization," *Research Square*, 2023. https://doi.org/10.21203/rs.3.rs-3204960/v1.

[15] S. Sivarao et al., "Predictive Modeling Of Dimensional Accuracies In 3d Printing Using Artificial Neural Network," *Journal of Engineering Science and Technology*, vol. 18, no. 4, 2023, pp. 2148-2160.

[16] S. Chinchanikar et al., "ANN modelling of surface roughness of FDM parts considering the effect of hidden layers, neurons, and process parameters," *Advances in Materials and Processing Technologies*, 2022. https://doi.org/10.1080/2374068X.2022.2091085

[17] F.M. Monticeli, R.M. Neves, H.L. Ornaghi Jr., and J.H.S. Almeida Jr., "Prediction of Bending Properties for 3D-Printed Carbon Fibre/Epoxy Composites with Several Processing Parameters Using ANN and Statistical Methods," *Polymers*, vol. 14, 2022, p. 3668. https://doi.org/10.3390/polym14173668.

[18] I. Milićević et al., "Improving the Mechanical Characteristics of the 3D Printing Objects using Hybrid Machine Learning Approach," *FACTA UNIVERSITATIS Series: Mechanical Engineering*, 2022. https://doi.org/10.22190/FUME220429036M.

[19] A.K. Gupta and M. Taufik, "Improvement of part strength prediction modelling by artificial neural networks for filament and pellet based additively manufactured parts," *Australian Journal of Mechanical Engineering*, 2022. https://doi.org/10.1080/14484846.2022.2047472

[20] M. Abas, T. Habib, S. Noor, B. Salah, and D. Zimon, "Parametric Investigation and Optimization to Study the Effect of Process Parameters on the Dimensional Deviation of Fused Deposition Modeling of 3D Printed Parts," *Polymers*, vol. 14, 2022. https://doi.org/10.3390/polym14173667.

[21] A.D. Tura, H.B. Mamo, Y.D. Jelila, and H.G. Lemu, "Experimental investigation and ANN prediction for part quality improvement of fused deposition modeling parts," *COTech & OGTech 2021*, IOP Conf. Series: Materials Science and Engineering, vol. 1201, 2021, p. 012031. https://doi.org/10.1088/1757-899X/1201/1/012031

[22] A. Dey and N. Yodo, "A systematic survey of FDM process parameter optimization and their influence on part characteristics," *J. Manuf. Mater. Process.*, vol. 3, no. 3, 2019, p. 64. https://doi.org/10.3390/jmmp3030064

[23] S.K. Padhi et al., "Optimization of fused deposition modeling process parameters using a fuzzy inference system coupled with Taguchi philosophy," *Adv. Manuf.*, vol. 5, 2017, pp. 231-242. https://doi.org/10.1007/s40436-017-0187-4

[24] V. Kumar and A. Kumar, "Improved bio bleaching of mixed hardwood pulp and process optimization using novel GA-ANN and GA-ANFIS hybrid statistical tools," *Bioresour. Technol.*, vol. 271, 2018, pp. 274-282. https://doi.org/10.1016/j.biortech.2018.09.115

[25] J.P. Patel, C.P. Patel, U.J. Patel, "A review on various approaches for process parameter optimization of fused deposition modeling (FDM) process and Taguchi approach for optimization," *International Journal Engineering Research and Application*, vol. 2, no. 2, 2012, pp. 361-5.

[26] J.M. Mercado-Colmenero et al., "A numerical and experimental study of the compression uniaxial properties of PLA manufactured with FDM technology based on product specifications," *Int J Adv Manuf Technol*, vol. 103, pp. 1893-1909, 2019. https://doi.org/10.1007/s00170-019-03626-0

[27] H.H. Abdulridha, T.F. Abbas, "Analysis and Investigation the Effect of the Printing Parameters on the Mechanical

and Physical Properties of PLA Parts Fabricated via FDM Printing," *Advances in Science and Technology Research Journal*, vol. 17, no. 6, 2023, pp. 49-62. https://doi.org/10.12913/22998624/173562

[28] S.A. Oudah, H.B. Al-Attraqchi, N.A. Nassir, "The Effect of Process Parameters on the Compression Property of Acrylonitrile Butadiene Styrene Produced by 3D Printer," *J. Eng. Technol.*, vol. 40, 2022, pp. 189-194. http://doi.org/10.30684/etj.v40i1.2118

[29] J.M. Zurada. *Introduction to Artificial Neural Systems*. St. Paul: West Publishing Company, 1992, pp. 1-764.

Hind H. Abdulridha (corresponding author)
ORCID ID: 0000-0003-4653-6073
University of Technology
Production Engineering and Metallurgy Department
Baghdad, Iraq
e-mail: Hind.H.Abdulridha@uotechnology.edu.iq

Tahseen F. Abbas
University of Technology
Production Engineering and Metallurgy Department
Baghdad, Iraq

Aqeel S. Bedan
University of Technology
Production Engineering and Metallurgy Department
Baghdad, Iraq